Chemical and Electrochemical Studies of $Cl_2FeS_2MS_2FeCl_2{}^{n-}$ Clusters [M = Mo (n = 2), W (n = 2), V (n = 3)]

Yanming Liu, Jinhai Chen, and Michael D. Ryan*

Chemistry Department, Marquette University, Milwaukee, Wisconsin 53233

The electrochemistry and spectroelectrochemistry of $[Cl_2FeS_2MS_2FeCl_2]^{n-}$ clusters (where n = 2 for M = Mo and W and n = 3 for M = V; **Ia**, **Ib**, and **Ic**, respectively) and the dimetal complex $[Cl_2FeS_2MoS_2]^{2-}$ (**IIIa**) were examined in order to characterize the structures and properties of the one-electron-reduced complexes. A stable reduction product for **Ia** was observed spectroelectrochemically at −1.05 V, which could be oxidized back to the starting complex. Reduction at more negative potentials caused complete bleaching of the spectrum, and the starting complex could not be obtained by reoxidation. Similar behavior was observed for the tungsten complex, **Ib**, but the dimetal complex $[Cl_2FeS_2WS_2]^{2-}$ was formed upon reoxidation. Chemical and electrochemical reduction of **Ia** and **Ib** both led to the same products (**IIa** and **IIb**), but by different mechanisms. Borohydride reduction of **Ia** and **Ib** led to the initial formation of the dimetal complex, while the electrochemical reduction of **Ia** proceeded by way of the formation of $[Cl_2FeS_2MoS_2FeCl_2]^{3-}$. Spectral changes were observed in the reduction of **Ic**, but they were not reversible. Resonance Raman spectroscopy of the reduced complexes was carried out in order to characterize the reduction product. Two polarized bands in the sulfur bridging region were observed in the resonance Raman spectra of electrochemically and chemically generated **IIa** and **IIb**. The relative intensities of these bands were dependent upon the excitation frequency. Reduction of **Ic** led to the loss of all resonance Raman bands. Reduction of **IIIa** gave rise to a complex (**IVa**) that was spectrally quite similar to **IIa**. These results, along with the previously reported result that the reduction complex was diamagnetic, indicate that the complex **IIa** is a dimeric species. The most likely structure consistent with these data is a $Mo_2Fe_2S_4$ cubane structure.

Introduction

The synthesis and characterization of clusters containing metals, bridged by sulfur, has been a fertile area of research. Many such clusters have been synthesized, and the current focus of this work has been the trimetal clusters of which two of the metal atoms are iron. Some members of this class include $[Cl_2FeS_2MS_2FeCl_2]^{n-}$, where M = Mo ($n$ = 2), W (n = 2), or V (n = 3) (**Ia**, **Ib**, and **Ic**, respectively). The X-ray structures and properties of these complexes have been reported by Coucouvanis[1] and Holm.[2] What has made the study of iron−sulfur and molybdenum−iron−sulfur cluster chemistry so fascinating is the range of reactions that can occur because of the lability of the complexes. Changes in solvent, metal, or ligand concentrations can produce significant changes in the structure and nuclearity of these clusters. These transformations have been well-documented for iron−sulfur[3−5] and molybdenum−iron−sulfur[6,7] clusters. While the effect of ligand and metal ratio has been studied in detail, changes due to oxidation or reduction have been examined to a lesser extent. For example,

Weterings et al.[8] have shown that the oxidation of 4Fe-4S clusters leads to a species that is spectroscopically similar to the 3Fe clusters in the 3Fe ferredoxins. The synthesis, structure, and properties of reduced 4Fe-4S clusters have also been examined.[9,10] Ciurli et al. have shown that reduction of linear three-iron clusters in the presence of nickel can yield a cubane.[11] Rosenhein et al. examined thiolate-bridged Mo−Fe and Mo−Co clusters, where a facile two-electron oxidation occurred, with the formation of new metal−metal bonds.[12,13]

The cyclic voltammetry of **Ia** and **Ib** has been reported,[14] along with some studies of the one-electron-reduced product. Significant efforts were spent, unsuccessfully, on trying to obtain X-ray-quality crystals of these complexes.[14] The empirical formula for the anion, though, was found to be $[MoFe_2S_4Cl_3]^{2-}$ (**IIa**). In addition to the empirical formula, the visible and infrared spectra along with the magnetic susceptibility were obtained. The compound was found to be diamagnetic, as was the starting complex, **Ia**, which, along with the voltammetric

(1) Coucouvanis, D.; Baenziger, N. C.; Simhom, E. D.; Stremple, P.; Swenson, D.; Simopoulos, A.; Kostikas, A.; Petrouleas, V.; Papaefthymiou, V. *J. Am. Chem. Soc.* **1980**, *102*, 1732−4.
(2) Do, Y.; Simhon, E. D.; Holm, R. H. *Inorg. Chem.* **1985**, *24*, 4635−42.
(3) Hagen, K. S.; Watson, A. D.; Holm, R. H. *J. Am. Chem. Soc.* **1983**, *105*, 3905−13.
(4) Hagen, K. S.; Reynolds, J. G.; Holm, R. H. *J. Am. Chem. Soc.* **1981**, *103*, 4054−63.
(5) Hagen, K. S.; Holm, R. H. *Inorg. Chem.* **1984**, *23*, 418−27.
(6) Coucouvanis, D. *Acc. Chem. Res.* **1981**, *14*, 201−9.
(7) Coucouvanis, D. *Acc. Chem. Res.* **1991**, *24*, 1−8.

(8) Weterings, J. P.; Kent, T. A.; Prins, R. *Inorg. Chem.* **1987**, *26*, 324−9.
(9) Hagen, K. S.; Watson, A. D.; Holm, R. H. *Inorg. Chem.* **1984**, *23*, 2984−90.
(10) Carney, M. J.; Papaefthymiou, G. C.; Frankel, R. B.; Holm, R. H. *Inorg. Chem.* **1989**, *28*, 1497−503.
(11) Ciurli, S.; Yu, S.-B.; Holm, R. H. *J. Am. Chem. Soc.* **1990**, *112*, 8169−71.
(12) Rosenhein, L. D.; Newton, W. E.; McDonald, J. W. *Inorg. Chem.* **1987**, *26*, 1695−702.
(13) Rosenhein, L. D.; Huffman, J. C. *Polyhedron* **1994**, *13*, 667−73.
(14) Coucouvanis, D.; Simhon, E. D.; Stremple, P.; Ryan, M.; Swenson, D.; Baenziger, N. C.; Simopoulos, A.; Papaefthymiou, V.; Kostikas, A.; Petrouleas, V. *Inorg. Chem.* **1984**, *23*, 741−9.

evidence, indicated a dimeric product.[14] A later report disputed this conclusion and described the product as one in which the cluster had been essentially destroyed.[15] In order to clarify the issues raised in that report, the reduction of the trimetal and dimetal complexes was probed using UV/visible and resonance Raman spectroscopy. The resonance Raman spectra of the linear Fe−Mo−Fe cluster,[16] Fe−Mo(W) complexes,[17−19] molybdenum proteins and models,[20] other molybdenum (tungsten) clusters,[21,22] and the starting tetrathiomolybdate and -tungstate[23,24] have already been obtained. Using these spectroscopic tools, the electrochemistry of a number of di- and trimetal sulfur-bridged complexes will be examined.

Experimental Section

Equipment. Cyclic voltammograms were obtained with an IBM Instruments EC/225 voltammetric analyzer with a Hewlett-Packard 7045A X-Y recorder. The reference electrode was a 0.1 M Ag/AgNO$_3$ electrode in acetonitrile. For comparison with literature data, all tabular data were converted to SCE values (E vs SCE = E vs Ag/AgNO$_3$ + 0.46 V). The working and auxiliary electrodes were platinum. The visible spectra were obtained with either a Perkin-Elmer 320 spectrophotometer equipped with a PE 3600 data station or a Hewlett-Packard 8452 diode array spectrophotometer. An optically transparent thin-layer electrochemical cell (OTTLE) was used for the visible spectroelectrochemical studies,[25] while a homemade three-electrode cell with an electrolysis volume of about 3−5 mL was used for controlled potential electrolysis and resonance Raman spectroelectrochemistry. The resonance Raman data were obtained on a Spex 1403 spectrometer with a photomultiplier detector. The laser sources were a Spectra-Physics 146 Kr$^+$ laser (412 nm) and an Ar$^+$ laser (488 and 514 nm).

Chemicals. The metal complexes (Ph$_4$P)$_2$[MoS$_4$Fe$_2$Cl$_4$], (Ph$_4$P)$_2$[Cl$_2$-FeS$_2$MoS$_2$], (Ph$_4$P)$_2$[WS$_4$Fe$_2$Cl$_4$], and (Me$_4$N)$_3$[VS$_4$Fe$_2$Cl$_4$] were synthesized by literature procedures.[1,2] Tetrabutylammonium perchlorate (TBAP) was obtained from GFS Chemical Co. Tetrabutylammonium tetrahydridoborate was purchased from Strem Chemical Co. Methylene chloride, dimethylformamide (DMF), and acetonitrile were obtained from Aldrich Chemical Co.

Procedures. All voltammetric solutions were deoxygenated by deaerating the solution for 15 min with prepurified dinitrogen. The dinitrogen was presaturated with the solvent in order to prevent evaporation. The coulometric and resonance Raman solutions were prepared in a glovebox under an argon atmosphere. The spectroelectrochemical data were obtained after the current had decayed to the background, except as noted in the text.

(15) Fabre, P. L.; deMontauzon, D.; Poilblanc, R. *Transition Met. Chem.* **1987**, *12*, 434−40.
(16) Muller, A.; Sarkar, S.; Dommrose, A.-M.; Filgueira, R. *Z. Naturforsch., B: Chem. Sci.* **1980**, *35b*, 1592−3.
(17) Müller, A.; Filgueira, R. R.; Jaegermann, W.; Che, S. *Naturwissenschaften* **1981**, *68*, 93−4.
(18) Clark, R. J. H.; Dines, T. J.; Proud, G. P. *J. Chem. Soc., Dalton Trans.* **1983**, 2299−302.
(19) Muller, A.; Jostes, R.; Toelle, H. G.; Trautwein, A.; Bill, E. *Inorg. Chim. Acta* **1980**, *46*, L121−4.
(20) Subramanian, P.; Burgmayer, S.; Richards, S.; Szalai, V.; Spiro, T. G. *Inorg. Chem.* **1990**, *29*, 3849−53.
(21) Clark, R. J. H.; Joss, S.; Zvagulis, M.; Garner, C. D.; Nicholson, J. R. *J. Chem. Soc., Dalton Trans.* **1986**, 1595−601.
(22) Halbert, T. R.; McGauley, K.; Pan, W.-H.; Czernuszewicz, R. S.; Stiefel, E. I. *J. Am. Chem. Soc.* **1984**, *106*, 1849−51.
(23) Clark, R. J. H.; Dines, T. J.; Wolf, M. L. *J. Chem. Soc., Faraday Trans. 2* **1982**, *78*, 679−88.
(24) Clark, R. J. H.; Dines, T. J.; Proud, G. P. *J. Chem. Soc., Dalton Trans.* **1983**, 2019−24.
(25) Lin, X. Q.; Kadish, K. M. *Anal. Chem.* **1985**, *57*, 1498−501.
(26) Tieckelmann, R. H.; Silvis, H. C.; Kent, T. A.; Huynh, B. H.; Waszczak, J. V.; Teo, B.-K.; Averill, B. A. *J. Am. Chem. Soc.* **1980**, *102*, 5550−9.
(27) Do, Y.; Simhon, E. D.; Holm, R. H. *J. Am. Chem. Soc.* **1983**, *105*, 6731−2.
(28) Müller, A.; Dommröse, A.-M.; Jaegermann, W.; Krickemeyer, E.; Sarkar, S. *Angew. Chem., Int. Ed. Engl.* **1981**, *20*, 1061−3.

Table 1. Cyclic Voltammetry of M−Fe−S Linear Clusters

complex	solvent	$E_{pc,I}$, V vs SCE	ref
[Cl$_2$FeS$_2$VS$_2$FeCl$_2$]$^{3-}$	DMF	−1.14	this work
[Cl$_2$FeS$_2$MoS$_2$FeCl$_2$]$^{2-}$	CH$_2$Cl$_2$	−0.60^a	this work
	CH$_2$Cl$_2$	−0.59	14
	CH$_2$Cl$_2$	−0.57	15
	CH$_3$CN	−0.55	15
	DMF	−1.05	this work
	DMF	−0.66	15
[Cl$_2$FeS$_2$WS$_2$FeCl$_2$]$^{2-}$	CH$_2$Cl$_2$	−0.90	this work
	CH$_2$Cl$_2$	−0.83	14
	DMF	−1.18	this work
[Cl$_2$FeS$_2$MoS$_2$]$^{2-}$	CH$_2$Cl$_2$	−1.19	15
	CH$_3$CN	−1.26	15
	CH$_3$CN	−1.2	19
	DMF	−1.38	15
	DMA	−1.33	26
[Cl$_2$FeS$_2$WS$_2$]$^{2-}$	CH$_3$CN	−1.3	19
[Mo$_2$Fe$_4$S$_8$Cl$_6$]$^{4-}$	DMF	−0.90	14

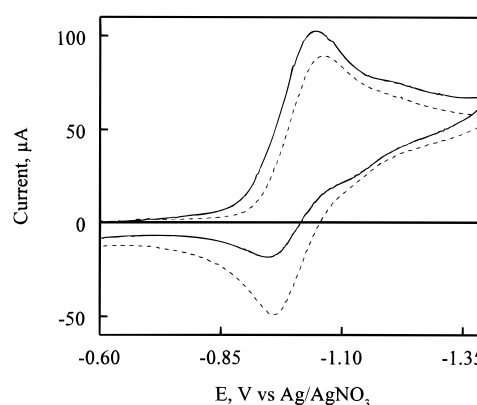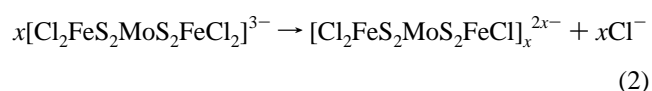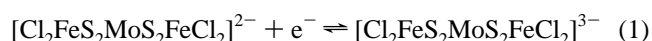^{a} Second wave at −0.76 V, irreversible.

Figure 1. Cyclic voltammetry of **Ia** in methylene chloride in the presence and absence of chloride ion. Concentration of **Ia** = 2.1 mM. Solid line: 0 mM chloride. Dotted line: 8.0 mM tetraphenylphosphonium chloride. Scan rate: 100 mV/s, 0.10 M TBAP. Reference electrode: Ag/AgNO$_3$ in acetonitrile.

Results and Discussion

Cyclic Voltammetry. The cyclic voltammetric data for the linear metal clusters are summarized in Table 1. The trimetal complexes became progressively more difficult to reduce as M was changed from Mo (*Ia*) to W (*Ib*) to V (*Ic*). Except for **Ia**, the waves were irreversible. The dimetal complexes, [Cl$_2$FeS$_2$MoS$_2$]$^{2-}$, **IIIa**, and [Cl$_2$FeS$_2$WS$_2$]$^{2-}$, **IIIb**, reduced in an irreversible wave between −1.2 and −1.4 V. The peak potentials for the molybdenum and tungsten dimetal complexes were about the same, under the same solvent conditions.

While a reverse peak was observed in the cyclic voltammetry of **Ia**, this complex showed evidence of an irreversible chemical reaction following the electron transfer. The overall stoichiometry for this reaction was shown to be[14]

$$[Cl_2FeS_2MoS_2FeCl_2]^{2-} + e^- \rightleftharpoons [Cl_2FeS_2MoS_2FeCl_2]^{3-} \quad (1)$$

$$x[Cl_2FeS_2MoS_2FeCl_2]^{3-} \rightarrow [Cl_2FeS_2MoS_2FeCl]_x^{2x-} + xCl^-$$
$$(2)$$

A close examination of the wave at slow scan rates also showed the appearance of a new cathodic wave at −1.22 V vs Ag/AgNO$_3$ (wave II) (Figure 1). The appearance of this new wave was concurrent with the decrease in the height of the reverse wave of the first reduction process, indicating that this
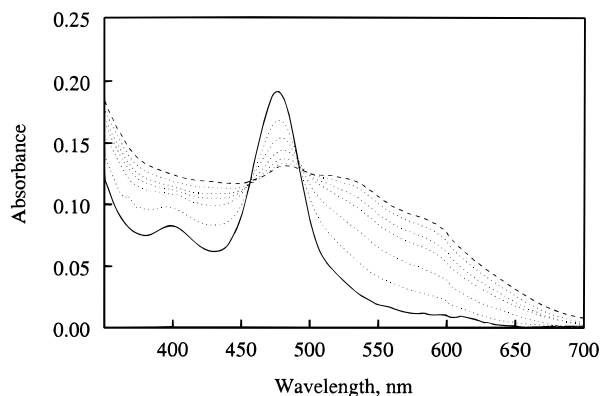
Figure 2. Thin-layer spectroelectrochemistry of **Ia** in methylene chloride. Concentration of **Ia** = 8 mM. Solid line: -0.60 V. Dotted lines: -0.90, -0.93, -0.96, -0.99, -1.02 V. Dashed line: -1.05 V vs Ag/AgNO$_3$ in acetonitrile. Concentration of TBAP: 0.20 M.

new wave was due to the Mo–Fe–S cluster formed by a chemical reaction after the electron transfer. Cyclic voltammograms of **Ia** in the presence of excess chloride ion showed that wave II was attenuated, and the reverse peak for wave I increased (Figure 1). This indicated a greater stability of **Ia**$^-$ with excess chloride present, probably due to the following equilibrium reaction:

$$[Cl_2FeS_2MoS_2FeCl_2]^{3-} \rightleftharpoons [Cl_2FeS_2MoS_2FeCl]^{2-} + Cl^-$$
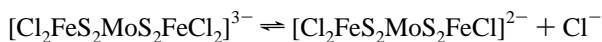
Unfortunately, the dissociation of **Ia** into [Cl$_2$FeS$_2$MoS$_2$]$^{2-}$ and FeCl$_4{}^{2-}$ limited the range of chloride concentrations that could be utilized.

The trimetal complex **Ia** is essentially dissociated into [Cl$_2$FeS$_2$MoS$_2$]$^{2-}$ (**IIIa**) and FeCl$_2$ in DMF.[1] In spite of the fact that **Ia** exists as the dimetal complex in DMF, **Ia** reduces more easily in that solvent than **IIIa**. In addition, an oxidation wave was observed in the reverse scan, indicating that the wave was, at least chemically, reversible. Such behavior would be consistent with a CE mechanism (chemical reaction prior to electron transfer), where complexation of **IIIa** by FeCl$_2$ occurs prior to reduction:

$$Cl_2FeS_2MoS_2{}^{2-} + FeCl_2 \rightleftharpoons Cl_2FeS_2MoS_2FeCl_2{}^{2-} \quad (3)$$
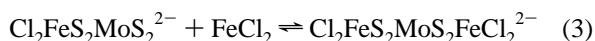
This equilibrium has been reported previously by Coucouvanis et al.[1] in DMF, where excess FeCl$_2$ can force the equilibrium to the right, converting the visible spectrum to the one observed for **Ia** in methylene chloride. The product of reaction 3 can then be reduced via reactions 1 and 2.
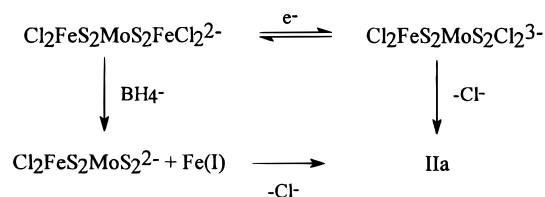
Oxidation of **Ia** in DMF gave rise to a series of oxidation waves at $+0.20$, $+0.34$, and $+0.61$ V. The first two waves appeared to be reversible with reverse peaks at $+0.26$ and $+0.12$ V and a broad peak at -0.4 V. Two waves (at $+0.23$ and $+0.58$ V) were observed for the oxidation of **Ic** in DMF, both of which were irreversible, and a broad reverse wave appeared at -0.4 V. In acetonitrile, the first oxidation wave for **Ic** was quasi-reversible, with an $E_{1/2}$ of $+0.12$ V.

Visible Spectroelectrochemistry. The visible spectroelectrochemistry of the three trimetal complexes, as well as **IIIa**, was examined using a thin-layer cell (OTTLE). For the molybdenum complex, the two strong bands at 475 and 398 nm disappeared, while a new band at 482 nm with shoulders at 513 and 582 nm appeared for the reduction product, **IIa**, obtained at -1.05 V (Figure 2). This spectrum was identical to the spectrum obtained by the coulometric reduction of **Ia**, but differed from the spectrum that had been reported previously

for **IIa** in DMF (Table 1). Reversal of the potential to -0.6 V led to regeneration of the original spectrum on both the OTTLE and controlled potential electrolysis time scale. The results are summarized in Table 2. Electrolysis in the region of wave II caused complete bleaching of the visible spectrum, and it was not possible to regenerate **Ia** at -0.6 V. This more negative potential was used by Fabre et al.[15] in their electrolysis of **Ia**. As long as the potential was positive of wave II, a stable colored complex was formed, which could be reoxidized to form the original **Ia** complex.

The spectroelectrochemical behavior of **Ia** in DMF was similar to that of methylene chloride. The position of the bands of **IIa** in DMF (Figure 3, curve B) was not significantly different from their position in methylene chloride (Figure 3, curve A), but the spectrum was not the same as the one reported for **IIa**.[14] The reasons for these differences will be discussed later. Reoxidation of **IIa** in DMF once again regenerated the original spectrum. Coulometric reduction of the dimetal complex **IIIa** at -1.25 V vs Ag/AgNO$_3$ in methylene chloride gave rise to a complex **IVa**, whose spectrum had four major bands in the visible (429, 468, 525, and 589 nm). This spectrum was very similar to that of **IIa**, but had relatively higher absorbances in the longer wavelength bands (Figure 3, curve C). Adjusting the potential 100 mV more negative (-1.35 V) caused further increases in the absorbances of the 525- and 589-nm bands, and the latter band moved to 600 nm (Figure 3, curve D). In general, electrolysis at more negative potentials or the use of dimetal complexes yielded products which absorbed more strongly in the 600–700-nm region, as well as shifting the lowest energy band to the red. The previously reported spectrum in DMF of **IIa** (see Table 1) was quite similar to the spectrum in Figure 3, curve D. It is difficult to control the solution redox potential within a narrow range with a strong reductant such as borohydride, making it very likely that the complex was over-reduced in the chemical reduction. Further evidence of this will be shown below in examining the kinetics of the borohydride–**Ia** reaction in methylene chloride.

While both the borohydride and electrochemical reduction of **Ia** led to **IIa**, the mechanisms for the reduction were surprisingly different. If the potential was stepped to -1.05 V, and the spectra were taken at 3-s intervals as the electrolysis was occurring (Figure 4), the formation of **Ia**$^-$ could be observed with good isosbestic points at 455 and 494 nm. The spectrum of **Ia**$^-$ was very similar to that of **Ia**, but the 475-nm band broadened and shifted slightly to 479 nm while its absorbance decreased. After 30 s (not shown in the Figure 4), a second phase was seen where the spectrum of **Ia**$^-$ disappeared and a new spectrum corresponding to **IIa** appeared. By contrast, the chemical reduction of **Ia** by borohydride led immediately (less than 4 s) to the formation of **IIIa**, which converted slowly to **IIa**. The two mechanisms are summarized below:

Cl$_2$FeS$_2$MoS$_2$FeCl$_2{}^{2-}$ $\overset{e^-}{\rightleftharpoons}$ Cl$_2$FeS$_2$MoS$_2$Cl$_2{}^{3-}$

$\downarrow$ BH$_4^-$ $\downarrow$ -Cl$^-$

Cl$_2$FeS$_2$MoS$_2{}^{2-}$ + Fe(I) $\xrightarrow{\text{-Cl}^-}$ **IIa**

The structure of the "Fe(I)" complex is not known, but because the reaction proceeds at stoichiometric ratios, the formation of **IIa** probably occurs by the reaction between **IIIa** and "Fe(I)". A close comparison of the visible spectra for the coulometric and chemical reductions indicates that borohydride

Table 2. Visible Spectra of M−Fe−S Clusters

complex	solvent	visible bands, nm (ϵ, mM^{-1} cm^{-1})	ref
[Cl$_2$FeS$_2$MoS$_2$FeCl$_2$]$^{2-}$	CH$_2$Cl$_2$	319 (13.9), 398 (4.4), 475 (9.89), 566 s, 600 (0.68)	14
	DMF	314 (12.2), 432 (4.07), 472 (5.8), 522 s, 600 s	1
[Mo$_2$Fe$_4$S$_8$Cl$_6$]$^{4-}$	CH$_2$Cl$_2$	482 (3.4), 513 s (3.2), 582 s (2.3)	this work
	DMF	429 (3.2), 473 (2.9), 520 s (2.5), 586 s (1.8)	this work
	DMF	432 (5.38), 530 (5.68), 580 (4.41)^a	14
[Cl$_2$FeS$_2$WS$_2$FeCl$_2$]$^{2-}$	CH$_2$Cl$_2$	294 (14.2), 360 (5.4), 418 (7.1), 502 (0.93)	14
[W$_2$Fe$_4$S$_8$Cl$_6$]$^{4-}$	CH$_2$Cl$_2$	362 (5.1), 426 (5.0), 502 (3.3)	this work
	DMF	346 (9.11), 414 (8.7), 430 (8.55), 510 (8.8), 555 s^a	14
[Cl$_2$FeS$_2$VS$_2$FeCl$_2$]$^{3-}$	CH$_3$CN	232 (32.1), 250 s, 310 (12.6), 350 s, 396 (5.5), 516 (6.4), 700s	27
[Cl$_2$FeS$_2$MoS$_2$]$^{2-}$	CH$_3$CN	290 (11), 314 (12.4), 432 (4.8), 469 (6.4), 528 s	26
reduced [Cl$_2$FeS$_2$MoS$_2$]$^{2-}$	CH$_2$Cl$_2$	428, 526, 590	this work
[Cl$_2$FeS$_2$MoS$_2$FeCl$_2$]$^{3-}$	CH$_2$Cl$_2$	395 (4.9), 479 (8.4)	this work

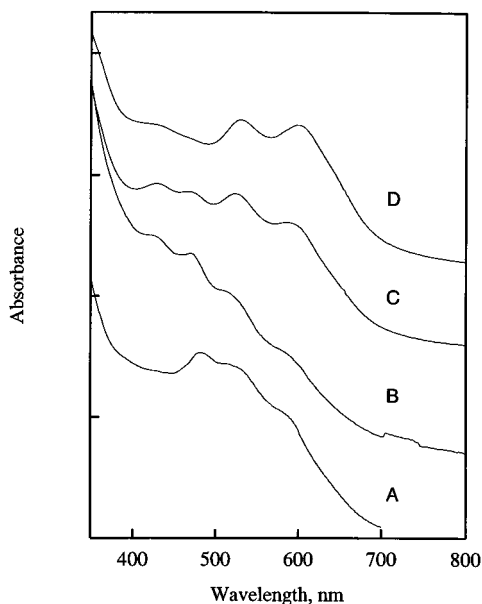^{a} Molar absorptivity based on empirical formula.

Figure 3. (A) Thin-layer spectroelectrochemistry of **Ia** in methylene chloride at −1.05 V. Concentration of **Ia** = 8 mM. (B) Thin-layer spectroelectrochemistry of **Ia** in DMF at −1.25 V. Concentration of **Ia** = 1.7 mM. (C) Coulometric reduction of **IIIa** in methylene chloride at −1.25 V. Concentration of **IIIa** = 1.2 mM. (D) Coulometric reduction of the solution in curve C at −1.35 V. Concentration of TBAP: 0.20 mM. Reference electrode: Ag/AgNO$_3$ in acetonitrile.

consistently over-reduces **Ia**, even before the complete conversion to **IIa** occurs.

Similar results were observed for the reduction of the tungsten analogue by borohydride. Immediately after mixing, the spectrum of the dimetal complex Cl$_2$FeS$_2$WS$_2$$^{2-}$, **IIIb**, was observed. A longer phase led to the formation of the ultimate product, **IIb**. Controlled potential electrolysis and OTTLE spectroelectrochemistry of **Ib** gave no evidence of **IIIb** or **Ib**$^-$. The spectrum of **IIb** was similar to that of **IIa**, but the bands were sharper and occurred at shorter wavelengths (see Table 1). The shift in the visible bands to shorter wavelengths with the replacement of Mo with W is consistent with the charge-transfer nature of the electronic transitions.[6] Reoxidation of **IIb** led to the regeneration of the dimetal complex **IIIb** rather than the trimetal starting complex **Ib**.

The spectral changes on the reduction of **Ic** in DMF were much more subtle than those observed for **Ia** and **Ib**. The band at 517 nm was attenuated and shifted to 510 nm while the 393-nm band became a shoulder. An isosbestic point was observed at 587 nm. The same spectrum could also be observed by reduction with borohydride. Reduction beyond −1.20 V led to a complete bleaching of the spectrum.
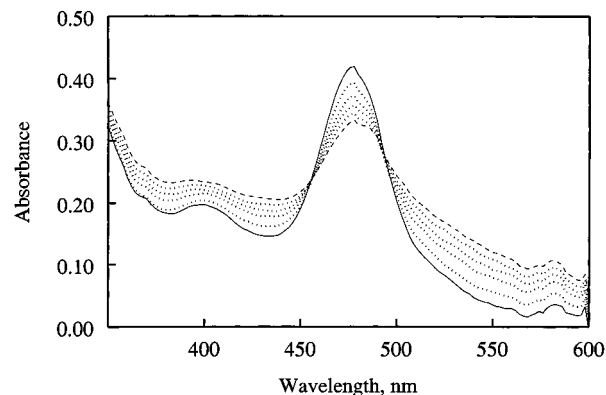

Figure 4. Thin-layer spectroelectrochemistry of **Ia** in methylene chloride obtained by stepping the potential to −1.05 V. Solid line: initial spectrum. Dashed line: spectrum after 24 s. Dotted lines: intermediate spectra after 10, 15, 18, and 21 s. Concentration of **Ia** = 1.0 mM; concentration of TBAP = 0.10 M. Reference electrode: Ag/AgNO$_3$ in acetonitrile.
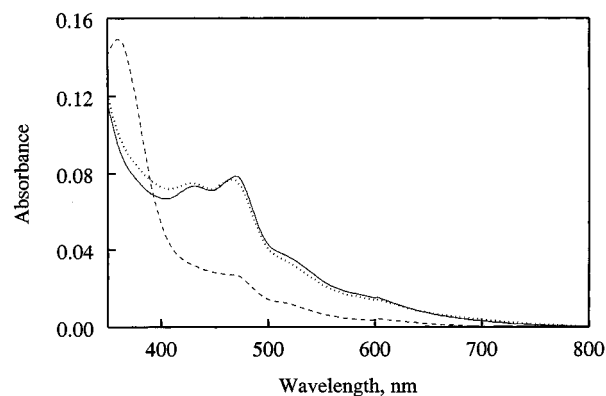

Figure 5. Thin-layer spectroelectrochemical oxidation of **Ia** in DMF. Concentration of **Ia** = 1.7 mM. Solid line: −0.60 V. Dashed line: +0.20 V. Dotted line: −0.80 V after oxidation at +0.20 V. All potentials vs Ag/AgNO$_3$ in acetonitrile. Concentration of TBAP: 0.20 M.

The oxidation of **Ia**, **Ib**, and **Ic** was also examined, and similar spectra were observed in all cases. The oxidation of **Ia** in DMF caused the absorbance of the 476-nm band to decrease, and a new band appeared at 355 nm (Figure 5). No spectral features due to tetrathiomolybdate nor **IIIa** could be observed. Similar results were observed in methylene chloride. Rereduction of this species almost completely regenerated the starting **Ia** complex (Figure 5). Oxidation of **Ib** and **Ic** in methylene chloride gave almost the same spectra (362 and 363 nm, respectively). Rereduction in these cases did not regenerate the original complexes. The oxidation of **Ic** was reversible on the

Table 3. Resonance Raman Spectra of M—S—Fe Linear Complexes

	Raman shift (cm^{-1})					
complex	ν_2, δ(M—S^b) [δ(M—S^t)]	ν_1, ν_s(M—S^b)	ν(M—S^t)	$\nu_1 + \nu_2$	$2\nu_1$	ref
[Cl$_2$FeS$_2$MoS$_2$FeCl$_2$]$^{2-}$ ^{a}	148	437		584	873	this work
	148	440		588	880	16, 17
reduced product^a	160/178	429/454				this work
reduced product^b	178	454			857	this work
[Cl$_2$FeS$_2$WS$_2$FeCl$_2$]$^{2-}$ ^{c}	143	459		600		this work
reduced product^c	160	454				this work
reduced product^a		443/454				this work
[Cl$_2$FeS$_2$MoS$_2$]$^{2-}$ ^{a}	148 [197]	426/429	489/493			this work
	158 [201]					17, 19
reduced product^a	157 [199]	427/454	481, 489			this work
[(PhS)$_2$FeS$_2$MoS$_2$]$^{2-}$ ^{d}		422/432	488			18
[(PhS)$_2$FeS$_2$WS$_2$]$^{2-}$ ^{d}		426/431	486/492			18
[Cl$_2$FeS$_2$VS$_2$FeCl$_2$]$^{3-}$	141	395		537	789	this work
(Ph$_3$P)AgS$_2$MoS$_2$Ag(PPh$_3$)		441/464				17
(Ph$_3$P)$_2$AgS$_2$MoS$_2$Ag(PPh$_3$)$_2$		443				28
[(PhS)CuS$_2$MoS$_2$]$^{2-}$		440/449	475/493			21
ClCuS$_2$MoS$_2$CuCl		430/446/468				21
[S$_2$MoS$_2$FeS$_2$MoS$_2$]$^{3-}$		414	479			this work

^{a} Laser excitation = 488 nm. ^{b} Laser excitation = 514 nm. ^{c} Laser excitation = 412 nm. ^{d} KBr disk; 70 K.

voltammetric time scale in acetonitrile, but on the longer time scale of OTTLE spectroelectrochemistry, only about 50% of the starting material could be regenerated upon rereduction. The spectrum of the oxidized product was the same as was observed in methylene chloride.

It is difficult to determine the oxidation state of the complex on the basis of the visible spectra. The fact that the wavelength of this band is almost invariant with the center metal (Mo, W, V) indicates that this transition probably involves a ligand to Fe charge transfer band. The S → Mo (V) charge transfer bands were attenuated in the oxidized complexes. A detailed examination of the oxidation chemistry for these complexes, though, was not carried out at this time.

Resonance Raman Spectroscopy. The resonance Raman spectra of the trimetal complexes that were studied were dominated by the symmetric M—S stretching ($\nu_{s,M-Sb}$) and bending (δ) vibrations (Table 3). Because of the high symmetry of these complexes, there was a series of relatively strong overtone and combination bands. The dimetal complexes had two stretching and bending bands, which corresponded to the M—S bridging ($\nu_{s,M-Sb}$) and the M-S terminal ($\nu_{s,M-St}$) vibrations.

Upon reduction, by either coulometric or chemical methods, a new resonance Raman spectrum was obtained. For 488-nm excitation, two new bands were observed at 429 and 454 cm^{-1}, while the band at 437 cm^{-1} and the combination and overtone bands at 584 and 874 cm^{-1} disappeared (Table 3). Oxidation of **IIa** regenerated the original **Ia**, again indicating the chemical reversibility of the redox reaction. Changing the excitation wavelength to 514 nm caused the 429-cm^{-1} band to increase in intensity, and a weak overtone band was now observed at 857 cm^{-1}. The 454-cm^{-1} band almost completely disappeared. Changes in the bending region are summarized in Table 3. Polarization studies of **IIa** showed that both the 429- and 454-cm^{-1} bands were polarized. The infrared bands for **IIa** have already been observed at 465 and 475 cm^{-1}.[14]

The resonance Raman spectrum of **IIIa** showed more subtle changes upon reduction to form **IVa**. The Mo—S stretching band at 489 cm^{-1} (Figure 6, curve A) broadened to give a shoulder at 481 cm^{-1} (Figure 6, curve B). The 426-cm^{-1} band increased in energy slightly to 427 cm^{-1}. A new band at 454 cm^{-1} was also observed. The biggest change was the shift in the bending Mo—S band from 148 to 157 cm^{-1}, while the 197-
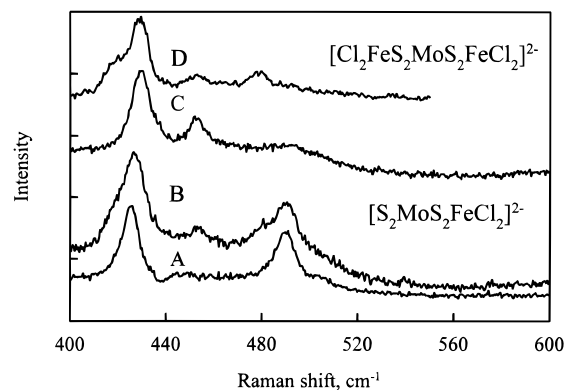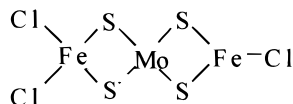

Figure 6. (A) Resonance Raman spectrum of **IIIa**. (B) Resonance Raman spectrum of the electrolysis product of **IIIa** at −1.25 V. (C) Resonance Raman spectrum of **Ia** electrolyzed at −1.05 V. (D) Resonance Raman spectrum of **Ia** electrolyzed at −1.05 V, followed by addition of tetraphenylphosphonium chloride. All solutions in methylene chloride with 0.10 M TBAP. Reference electrode: Ag/AgNO$_3$ in acetonitrile.

cm^{-1} band increased slightly to 199 cm^{-1}. Comparison with **IIa** (Figure 6, curve C) showed similarities and differences. Two bands around 430 and 454 cm^{-1} were observed for both reduced complexes, but **IIa** lacked the Mo—S terminal stretching band which was present in **IVa**. Addition of chloride ion to the **IIa** solution (Figure 6, curve D), though, caused the Mo—S stretching band to appear at 479 cm^{-1}. The 178-cm^{-1} bending band also disappeared, and new bands at 158 and 197 cm^{-1} appeared (not shown in Figure 6). An examination of curves B and D of Figure 6 shows that the pattern of Raman shifts is the same for both solutions.

The results for the tungsten complex, **IIb**, were similar to those for the molybdenum complex (Table 3). With 413-nm excitation, the 459-cm^{-1} band decreased slightly to 454 cm^{-1}. If the excitation wavelength was changed to 514 nm, two bands were observed at 443 and 454 cm^{-1}. The bending vibrations were too weak to be unambiguously identified. No resonance Raman spectrum was observed for the coulometrically reduced **Ic**. This does not necessarily mean that the complex was totally destroyed. It may be that the intensities of the bands were too low to be observed. In the case of molybdenum and tungsten complexes, there was a significant attenuation of the resonance Raman signal upon reduction of the complex.
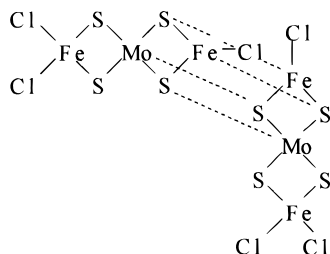
While there was considerable loss of symmetry in the formation of **IIa**, some symmetry was still maintained, at least on a local level. This was indicated by the presence of overtone bands under some conditions, and the fact that the infrared and Raman bands appeared at different frequencies. The lack of extensive overtone and combination bands excludes the monomeric structure:

Such a structure, which maintains high local symmetry, should give rise to strong overtone and combination bands.[17,29] In addition, this structure should be paramagnetic, while **IIa** is diamagnetic.

Other dimeric structures as proposed previously[14] are less likely on the basis of the spectroscopic data and the known bonding properties of iron and molybdenum. Reduction of Fe^{II} to Fe^{I} should lead to a decrease in coordination number, which is probably the driving force for the loss of chloride ion from **Ia**$^-$. Thus a structure with tetravalent iron containing two bridging chlorine atoms is not as favorable.[14] A second dimeric structure involved triply bridging sulfur atoms. Complexes of Mo$-$S$-$Cu have been synthesized with triply bridging sulfur, but the metal$-$sulfur vibrations of these complexes were observed in both the infrared and Raman spectra[21] due to their lower symmetry.

Another dimeric structure that has not yet been considered is a cubane structure with a Mo$_2$Fe$_2$S$_4$ core. This structure can be obtained (formally) by the two bridging sulfurs of one **Ia**$^-$ attacking the molybdenum and iron atoms of a second molecule (and vice versa).


If we assume that the irons are in the $+2$ oxidation state and the molybdenums are $+5$, we can satisfy the expanded coordination geometry of molybdenum and maintain the iron in the ferrous state. The dimerization of **IIIa** should lead to the same cubane, without the complexing FeCl$_2$ groups. The ease by which **IIa** is oxidized back to **Ia** is consistent with the above structure. Cleavage of the cubane along the plane between the two monomers and the addition of chloride ion will reconstitute **Ia**. Such a cleavage has already been reported by Coucouvanis et al.[30] for a double cubane MoFe$_3$S$_4$ cluster, which decomposed upon oxidation to two MoS$_2$Fe fragments. Oxidation of the presumed **IIb** reduction product would lead initially to Cl$_2$FeS$_2$WS$_2$FeCl^{2-}. This complex was probably less stable than the molybdenum analogue and decomposed before the addition of chloride. As a result, the observed reoxidation product was the dimetal complex **IIIb**.

The spectroscopic and chemical properties of **IIa** are consistent with this structure. The cubane contains two different types of bridging sulfur atoms, one associated with two Mo atoms and one Fe, and a second associated with one Mo and two Fe. These different bridging sulfurs may be the origin of the two bridging sulfur bands. There have been few infrared or Raman studies of Fe$-$M$-$S cubanes, but the vibrational frequencies are consistent with such a structure. The infrared vibration for Fe(μ_3-S) has been observed at 450 cm^{-1} for an Fe$-$Mo cluster,[31] while the ν(M$-\mu_3$S)/ν(Cu$-\mu_3$S) vibrations for M$_3$CuS$_4$ cubanes (where M = Mo or W) were observed between 400 and 450 cm^{-1}.[32$-$34] Both bands were observed in the resonance Raman spectra of **IIa** and **IVa**. The external Mo$-$S$-$Fe band cannot be unambiguously identified due to the broadness of the bands, especially around 430 cm^{-1}.

When chloride is added to **IIa**, it should be possible to remove the coordinated ferrous chloride groups.

$$[Mo_2S_8Fe_2Cl_2](FeCl_2)_2{}^{4-} + 8Cl^- \rightleftharpoons$$
$$[Mo_2S_8Fe_2Cl_2]^{4-} + 2FeCl_4{}^{2-}$$
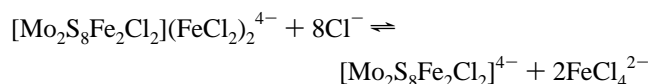
As evidence for this reaction, terminal Mo$-$S stretching bands were observed when chloride was added to a solution of **IIa** as shown in Figure 6, curve D. This facile interconversion between **IIa** and **IVa** provides strong evidence for this proposed structure.

The bonding in linear Mo$-$Fe$-$S clusters has been examined by Liu et al.,[35] and by Szterenberg and Jeżowska-Trzebiatowska.[36] Metal$-$metal bonding between Mo$-$Fe was predicted for **Ia** via the 2e orbitals (d$_{z^2}$, d$_{xy}$) of Mo with the 2e orbital of Fe.[35] This would result in two Mo$-$Fe bonds (one with each iron) and two non-interacting high-spin Fe atoms, coupled antiferromagnetically. Reduction of this complex would result in the addition of an electron to a nonbonding iron orbital (the empty Mo 4t$_2$ orbitals have significantly higher energy), yielding a formal iron(I) oxidation state. For other complexes such as a related trimetal complex, S$_2$MoS$_2$FeS$_2$MoS$_2{}^{3-}$, the formal Fe-(I) charge was minimized by the formation of two Mo$-$Fe bonds.[35] While the addition of an electron may strengthen the back-bonding of the Fe into the Mo 2e orbitals, no additional bonds would be formed, and the Mo$-$Fe bond in **Ia** is, in any case, relatively weak. As a result of this formal Fe(I) oxidation state, it is easy to understand the ease of the loss of Cl$^-$ in **Ia**$^-$. This open coordination site would favor dimerization to a cubane, which would shift the reduction site from Fe to Mo (Mo in the cubane would be $+5$).

A similar analysis of the molecular orbital level of **I** would predict that the oxidation would be centered on the iron atom. The sulfur bridges are susceptible to further oxidation, which is probably the source of the irreversibility. The HOMO orbitals of **I** are the nonbonding d orbitals of iron. There was no spectral evidence for the dimetal complexes **III**, and the reversibility of the cyclic voltammetric wave under some conditions would indicate that the iron did not cleave from the complex. This would be the first evidence for a ferric ion complexed with a tetrathiomolybdate.

(29) Müller, A.; Diemann, E.; Jostes, R.; Bögge, H. *Angew. Chem., Int. Ed. Engl.* **1981**, *20*, 934$-$955.

(30) Coucouvanis, D.; Alahmad, S.; Kim, C. G.; Mosier, P. E.; Kampf, J. W. *Inorg. Chem.* **1993**, *32*, 1533$-$5.

(31) Jordanov, J.; Hendriks, H. M.; Dupre, N.; Viari, A.; Vigny, P.; Diakun, G. *Inorg. Chem.* **1988**, *27*, 2997$-$3000.

(32) Zheng, Y.; Zhan, H.; Wu, X.; Lu, J. *Transition Met. Chem.* **1989**, *10*, 161$-$4.

(33) Zhan, H.; Zheng, Y.; Wu, X.; Lu, J. *Inorg. Chim. Acta* **1989**, *156*, 277$-$80.

(34) Wu, X.; Lu, S.; Zu, L.; Wu, Q.; Lu, J. *Inorg. Chim. Acta* **1987**, *133*, 39$-$42.

(35) Liu, C. W.; Lin, Z. Y.; Lu, J. X. *THEOCHEM* **1988**, *49*, 189$-$208.

(36) Szterenberg, L.; Jeżowska-Trzebiatowska, B. *J. Organomet. Chem.* **1989**, *371*, 361$-$70.

Conclusions

There is considerable precedent for the transformation of linear Mo−Fe−S structures into cubanes. Such a transformation enables the molybdenum atom to attain a lower oxidation state, as compared to its linear counterpart.[37,38] Cubanes of molybdenum with a $Mo_2M_2S_4$ structure have been identified where M = Co,[39] Cu,[40] or Fe.[41] The latter complex utilized dithiocarbamate ligands, with a +5 core, very similar to the core proposed in this work (+6).

The differences in the reduction pathways for the chemical and electrochemical processes indicate that the final products, **IIa** and **IIb**, were the thermodynamically favored species because the two reduction mechanisms led to the same products. The final products of the reduction were very dependent upon the applied potential or the strength of the reductant. More negative potentials are capable of reducing **IIa** or **IIb** and leading eventually to the products observed by Fabre et al.[15]

(37) Cheng, W.; Zhang, Q.; Huang, J.; Lu, J. *Jiegou Huaxue* **1990**, *9*, 243−8.

(38) Liu, Q.; Huang, L.; Liu, H.; Lei, X.; Wu, D.; Kang, B.; Lu, J. *Inorg. Chem.* **1990**, *29*, 4131−7.

(39) Halbert, T. R.; Cohen, S. A.; Stiefel, E. I. *Organometallics* **1985**, *4*, 1689−90.

(40) Zhu, N.; Zheng, Y.; Wu, X. *J. Chem. Soc., Chem. Commun.* **1990**, 780−1.

(41) Xu, J.; Qian, J.; Wei, Q.; Hu, N.; Jin, Z.; Wei, G. *Inorg. Chim. Acta* **1989**, *164*, 55−8.

The results of these electrochemical and spectroscopic studies indicate the ease by which these Mo−Fe clusters can rearrange in a reversible manner upon changes in oxidation state. It is important to note that the overall chemical reversibility cannot be always predicted from cyclic voltammetric results. Slow chemical steps, which often occur with these complexes, may not be observed. The ease of these transformations emphasizes the importance of protein structure on stabilizing a particular cluster that may have to undergo redox changes. This is of particular importance to nitrogenase, which contains a relatively large Mo−Fe−S cluster. Unlike heme proteins, where the structure is relatively well defined by the organic ligand, the stability of a given Mo−Fe−S or Fe−S structure is quite dependent upon oxidation state and coordination. Studies in recent years have shown the variety of stable structures that can be formed, and it is clear that the protein must be designed to maintain a fixed structure during the catalytic cycle. Further work will be pursued on the generality of the linear to cubane conversions upon reduction.